THE ASTROPHYSICAL JOURNAL, 312:134–142, 1987 January 1

CENTAURUS A OBSERVATION AT MeV–GAMMA-RAY ENERGIES

P. VON BALLMOOS, R. DIEHL, AND V. SCHÖNFELDER
Max-Planck-Institut für extraterrestrische Physik, Garching
Received 1986 April 1; accepted 1986 June 27

ABSTRACT

γ-ray emission above 700 keV from the direction of Centaurus A was detected during a balloon flight with the MPI Compton telescope. The statistical significance of the source detection is 4.1 σ. The location of the source, the profile of the derived source image, and the intensity and shape of the derived energy spectrum strongly suggest that the detected radiation is related to Cen A. The energy spectrum extends into the MeV range at least up to 8 MeV and connects well to the power-law spectrum, which so far has been measured up to several hundred keV. If the upper limits from *SAS 2* and *COS B* for γ-ray emission above 35 MeV and 50 MeV respectively were valid also during the balloon flight, the spectrum must steepen rapidly at energies around 10 MeV. No γ-ray lines have been found in the spectrum. The derived 2 σ upper limits on line emission are below previously reported line intensities. The hard X-ray/soft γ-ray spectrum can be interpreted as a thermal Comptonization spectrum with the parameters $kT_e = 5.1$ MeV and $\tau_T = 0.15$. For the special case of pair equilibrium, a lower limit to the source radius of 2.5×10^{14} cm can be derived. The spectrum also fits the two-component synchrotron–self-Compton model of Grindlay.

Subject headings: galaxies: individual — gamma rays: general — radiation mechanisms

I. INTRODUCTION

The bright radio galaxy Cen A (NGC 5128) is the nearest active galaxy, at a distance of ~ 5 Mpc. It was one of the first extragalactic objects to be identified as an X-ray emitter (Bowyer *et al.* 1970). During the last 10 years, several observations at hard X-ray ($E_X > 10$ keV) and low γ-ray energies have shown that the energy spectrum of Cen A is of the power-law type up to at least several hundred keV (Mushotzky *et al.* 1976; Hall *et al.* 1976; Mushotzky *et al.* 1978; Baity *et al.* 1981; Pietsch *et al.* 1981; Gehrels *et al.* 1984). At these energies Cen A is highly variable on the time scale of months in intensity as well as in spectral slope.

Observations at γ-ray energies by *SAS 2* above 35 MeV (Bignami *et al.* 1979) and *COS B* about 50 MeV (Pollock *et al.* 1981) yielded only upper limits on its emission. An observation with the balloon-borne telescope of Rice University (Hall *et al.* 1976) at low γ-ray energies resulted in an upper limit to the continuum emission above 1 MeV and in the detection of two γ-ray line features near 1.6 MeV and 4.4 MeV. At ultra-high γ-ray energies, Grindlay *et al.* (1975) have reported a positive detection of Cen A above 100 GeV, which was based on the ground-based Cerenkov technique.

The flat shape of the power-law spectrum of Cen A at X-ray energies and the existing limits to its flux at γ-ray energies above 35 MeV suggest that its maximum of luminosity should lie somewhere in the MeV range. Observations at MeV energies are therefore expected to contribute significantly to our understanding of the primary source mechanism of this active galaxy. The observed variability suggests that the source is rather small in volume, but its nature is still unclear.

In this paper an observation of γ-ray emission from the direction of Cen A in the energy range between 0.7 and 20 MeV is described. The observation was made during a balloon flight with the MPI Compton telescope (Schönfelder, Graser, and Diehl 1982). The balloon flight was performed from Uberaba, Brazil, on 1982 October 31 under very difficult conditions. It ended after only 4.5 hr at float, due to a balloon failure (3.5–4 g cm^{-2} residual atmosphere). Cen A was within the field of view of the telescope, but at large angular distances between 23° and more than 50° to the telescope axis. Therefore, no full use of the telescope sensitivity could be made. The maximum detection efficiency of the telescope is obtained for angles of incidence close to the axis. At the end of the flight the galactic center came into the field of view. This part of the flight was excluded from the present analysis and is investigated separately (von Ballmoos, Diehl, and Schönfelder 1986).

The telescope and details of the balloon flight are described in § II. The data analysis approach (different from the one used by Schönfelder, Graser, and Diehl 1982) is described in § III. In § IV the results of the analysis are summarized, including the significance of the source detection, the derived γ-ray flux and the energy spectrum. Arguments for the identification of the observed source with Cen A are given. The energy spectrum does not yet allow firm conclusions on the radiation mechanism involved because of too large statistical uncertainties and because of the lack of correlated observations in other spectral ranges. Possible interpretations of the energy spectrum and restrictions derived from the spectrum are described in § V.

II. OBSERVATIONS

A detailed description of the telescope and its properties is given by Schönfelder, Graser, and Diehl (1982). The telescope consists of two large area scintillation detectors, an upper one (D1) of liquid scintillator NE 213 and a lower one (D2) of NaI(Tl). Both detectors are entirely surrounded by an anticoincidence shield of plastic scintillator. An incident γ-ray is identified by two successive interactions: it is Compton-scattered in the upper detector system and thereafter absorbed in one of the modules of the lower detector. In each detector layer the position of the interaction and the energy deposit of the event is measured. Additional measurements (in order to reduce the number of background events) are the time of flight of the scattered γ-ray from D1 to D2 and the pulse shape in D1, which allows rejection of neutron induced events.

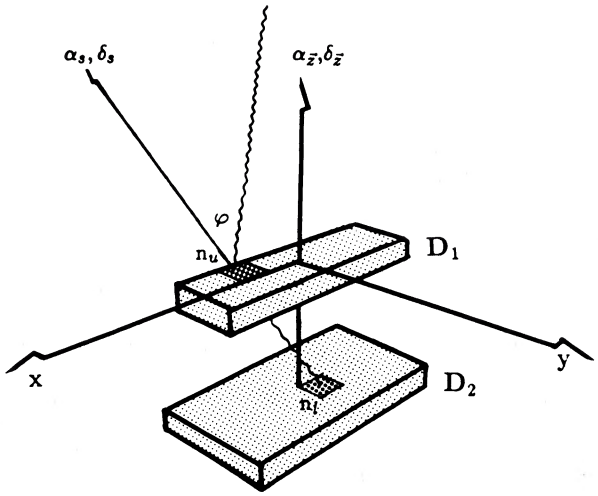

FIG. 1.—Schematic view of the telescope

Figure 1 shows a schematic view of the instrument. The essential event parameters are the time-dependent orientation of the telescope with respect to the sky, the direction of the scattered γ-ray in the detector system (θ, ϕ), and the energy deposits E_1 and E_2 in the two detectors. From the two energy deposits a "derived scatter angle" $\bar{\varphi}$ can be calculated according to

$$\cos \bar{\varphi} = 1 - \frac{m_e c^2}{E_2} + \frac{m_e c^2}{E_1 + E_2}, \quad (1)$$

with $m_e c^2 = 511$ keV.

The derived scatter angle $\bar{\varphi}$ is identical to the true Compton scatter angle φ, if the event parameters are measured without systematic errors (e.g., if the scattered γ-ray E_γ^s is totally absorbed in D2). The information on the arrival direction of the incident γ-ray is a function of the six parameters (E_1, E_2, α_s, δ_s, θ, ϕ), where the telescope orientation is translated into the projection of the scatter direction onto the sky in equatorial coordinates (α_s, δ_s).

The telescope has a field of view of typically 40°–60° FWHM, which is slightly energy-dependent and which can be modified in the analysis by certain event selection criteria. The telescope angular resolution is a function of the source position with respect to the telescope axis. For positions near the axis the 1 σ angular profile of a point source is 3°.5. At larger off-axis angles the profile becomes asymmetric and its width ranges from 3°.5 to 9°.

During the balloon flight the telescope was suspended in such a way that the telescope axis always pointed toward the zenith. The instantaneous azimuthal orientation was derived from two magnetometers and a Sun sensor to within $\pm 1°$. Two inclinometers were used to monitor deviations of the (x, y)-telescope plane from the horizontal plane. All flight data were electronically transmitted to the ground and stored on magnetic tapes.

The region of the sky observed during the balloon flight is shown in Figure 2 along with the track of the balloon. The balloon had reached its float altitude of 3.5 g cm^{-2} at 14:30 UT, a few minutes after the transit of Cen A. After 17:00 UT, telemetry problems arose which resulted in a loss of $\sim 50\%$ of the data after that time. At 18:55 UT the flight had to be terminated, due to the balloon failure. The data analysis of the present paper is based on data from the time interval 13:30 UT to 17:08 UT only.

We summarize the symbols used in this article:

E_γ	energy of the infalling γ-ray
E_γ^s	energy of the scattered γ-ray
D_1/D_2	upper detector/lower detector

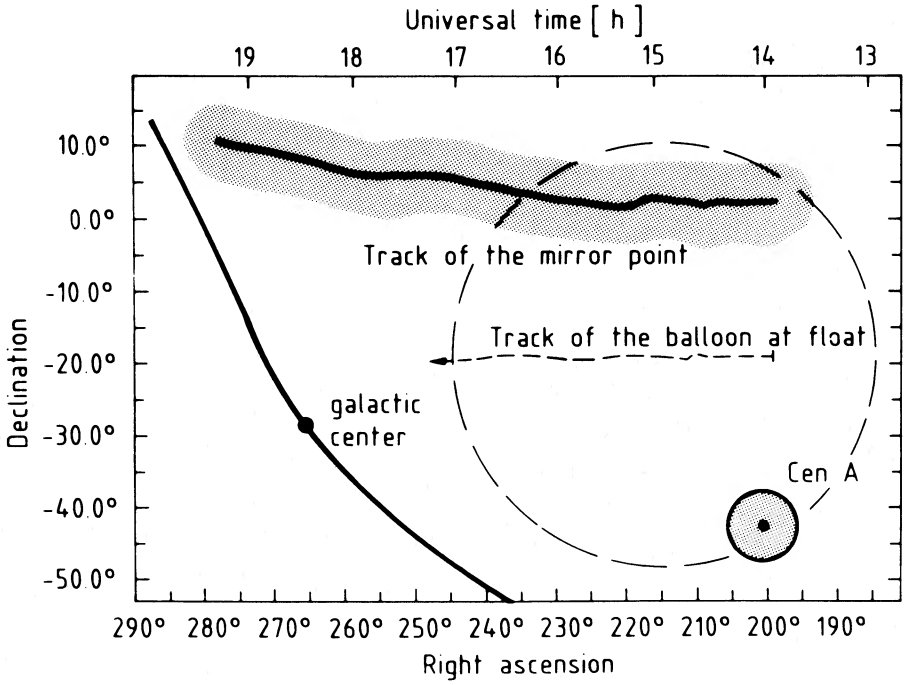

FIG. 2.—Part of the sky which was observed during the balloon flight. The track of the balloon at ascent (*dashed line*) and at float (*solid line*) is shown. The large circle indicates the field of view of the telescope (FWHM). Also shown is the track of the mirror point of Cen A between 13:30 UT and 17:08 UT.

E_1/E_2	energy loss in the upper/lower detection system
φ	true scatter angle in D_1
$\bar{\varphi}$	derived scatter angle (from eq. [1])
n_u/n_l	hidden detector block in D_1/D_2
θ/ϕ	scatter direction in the telescope system (zenith/azimuth angle)
α_s/δ_s	scatter direction in the equatorial system (right ascension/declination)
α_z/δ_z	telescope axis in the equatorial system

III. DATA ANALYSIS

A Compton telescope has imaging properties within a wide field of view. It is at present the only telescope that has proven imaging capabilities at MeV energies. An earlier sky map method used by Graser and Schönfelder (1982) to derive an image of the anticenter region of the galaxy with the same telescope was based on the idea that the arrival direction of an incident γ-ray should lie on an "event circle"—a circle of radius $\bar{\varphi}$ that is centered at (α_s, δ_s). In this case for each bin of the sky which is intersected by such a circle a certain probability can be calculated that the photon originally came from that bin. In order to generate a brightness distribution, the event circles of all accepted events are projected onto the celestial sphere. The brightness within a certain sky bin is then derived by adding up the probabilities of all event circles intersecting this bin. Background is subtracted by modeling the "exposure" of each sky bin taking into account the telescope efficiency.

For the present analysis a new method was developed which shows advantages in sensitivity, source location, and background treatment. This method which we call the π-method is characterized by three main features: event matrices, the mirror method, and likelihood ratio skymaps.

a) Event Matrices

The $\bar{\varphi}$-event circle is replaced by a two-dimensional matrix which contains the probabilities $dp^{(j)}(\alpha, \delta)$ that the jth photon originally came from the direction of bin (α, δ). For any set of event parameters (E_1, E_2, α_s, δ_s, θ, ϕ)—and hence for each detected γ-ray event—a probability matrix can be constructed. Figure 3 shows a typical example together with the corresponding event circle. The shape of the matrix (looking like a doughnut) slightly depends on the energy spectrum of the incident γ-rays. The probability matrices were determined by means of a Monte Carlo program: the detection of isotropically incident γ-rays with an $\sim E^{-2}$ differential photon number spectrum was simulated, and for each set of parameters of the detected events the distribution of the actual arrival directions was determined. In the special example of Figure 4 the 4° offset between the $\bar{\varphi}$-circle and the ridge of the distribution is typical for a Compton telescope; it is due to the fact that the event parameters cannot be measured without systematic errors. In some cases the scattered γ-ray is only Compton-scattered in D2 and not totally absorbed; this results in a $\bar{\varphi}$-value larger than the actual scattering angle. For other events the calculated $\bar{\varphi}$-value is too small due to the influence of energy thresholds. The event probability matrices take into account these systematic errors, unlike the previously used event circles.

b) Mirror Method

The mirror method is a simple and efficient tool for determining the background distribution from the flight data themselves. The instrument symmetry allows us to define for each source another direction (mirror source) which has the same efficiency and atmospheric depth for incident photons. The mirror direction of a celestial source has the same zenith angle

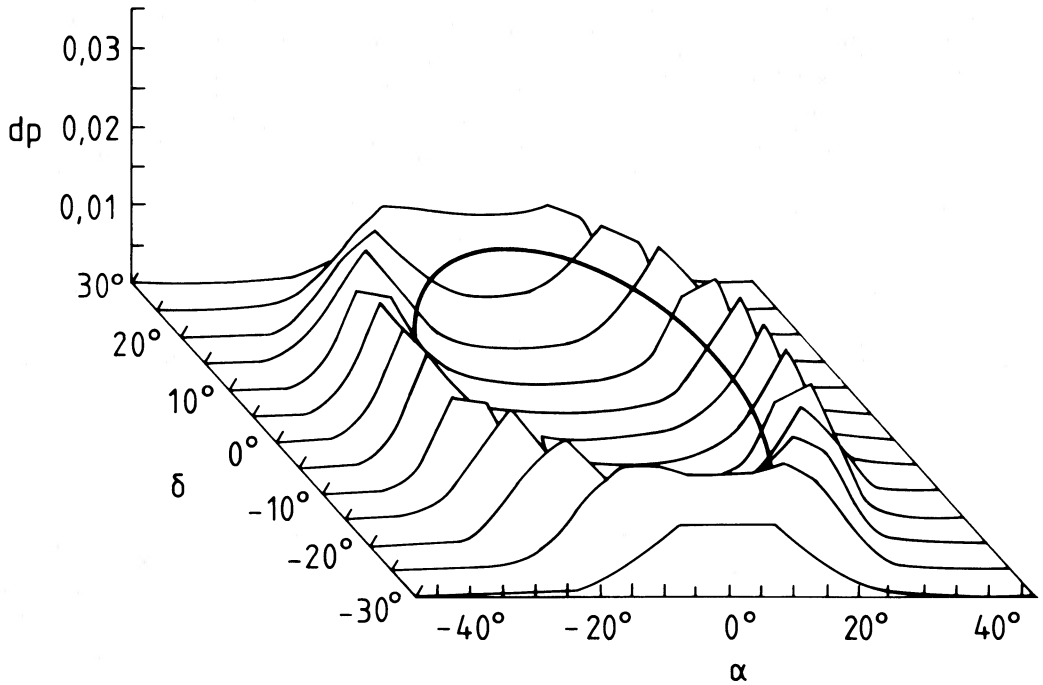

FIG. 3.—Example of probability matrix $dp^{(j)}(\alpha, \delta)$ for an event with $E_1 = 0.214$ MeV and $E_2 = 1.097$ MeV. Also shown is the event circle ($\bar{\varphi} = 22.^{\circ}5$).

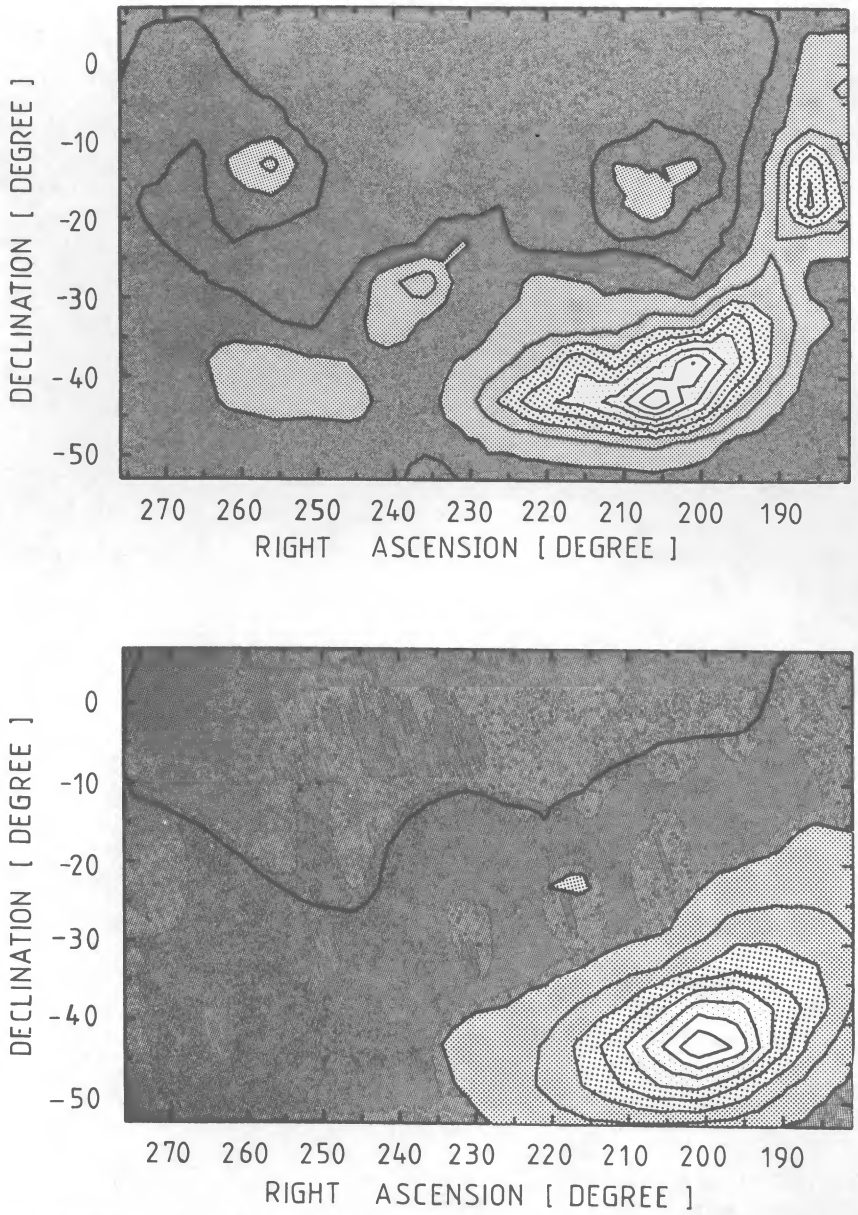

FIG. 4.—Skymap of equidistant likelihood contour lines (in steps of 10% of the maximum value) derived from all events in the range 0.7–20 MeV satisfying $\bar{\varphi} < 37°$. (*top*) Map derived from balloon flight data. The likelihood maximum for the existence of a source is at $\alpha = 206°$, $\delta = -43°$. (*bottom*) Result of a Monte Carlo simulation of the balloon flight under the assumption that Cen A is the only γ-ray source in the sky.

as the source, but its azimuthal angle is rotated by 180°. During the balloon flight the mirror direction of a source moves over the sky due to Earth's rotation and the movement of the balloon. (The track of the mirror point of Cen A during our balloon flight is indicated in Fig. 2). This technique of background treatment has similarities with the ON and OFF technique used in X-ray observations, except that our ON and OFF observations are performed simultaneously, due to the large field of view of the telescope.

Instead of comparing arrival direction probabilities of the measured events at a source and its mirror position, it is equivalent to define for each *real* event a *virtual* event whose scatter direction is the real event's scatter direction rotated by 180° in azimuth angle. We then compare the arrival direction probabilities of all real and virtual photons at the celestial source position.

The mirror method compensates for all fluctuations due to balloon altitude, cutoff rigidity, and data gaps automatically, thus easing background treatment. The method is based on the assumption that the background is isotropic and that the telescope response indeed is symmetrical with respect to the instrumental (X, Z)- and (Y, Z)-plane. Minor asymmetries of the telescope (differences in gains or thresholds) are smeared out by the rotation of the balloon during flight.

c) *Likelihood Ratio Skymap*

In order to derive a map of the sky, one can compare arrival direction probabilities from all possible directions of the

observed sky region with the corresponding probabilities of the virtual sky. This comparison is done by means of the π-method.

Whereas the event circle method forms the sum of probabilities per bin, the π-method forms the product of probabilities per bin. The probability that N measured events originated from a certain direction (α, δ) is

$$P_r(\alpha, \delta) = \prod_{j=1}^{N} dp_r^{(j)}(\alpha, \delta) \,. \tag{2}$$

Because of the high background, most events typically contribute $dp_r \approx 0$; therefore we use the complementary probabilities

$$\overline{dp_r}(\alpha, \delta) = 1 - dp_r^{(j)}(\alpha, \delta) \tag{3}$$

to derive the corresponding product $\overline{P_r}(\alpha, \delta)$. This is the likelihood that none of the N detected *real* events originated from bin (α, δ). $\overline{P_v}(\alpha, \delta)$ is the corresponding likelihood for the background: it describes the probability that none of the *virtual* events originated from bin (α, δ). The π-skymap brightness $\overline{Q}(\alpha, \delta)$ is defined by the ratio of two likelihoods:

$$\overline{Q}(\alpha, \delta) = \frac{\overline{P_v}(\alpha, \delta)}{\overline{P_r}(\alpha, \delta)} = \frac{\prod_{i=1}^{N} [1 - dp_v^{(j)}(\alpha, \delta)]}{\prod_{j=1}^{N} [1 - dp_r^{(j)}(\alpha, \delta)]} \,, \tag{4}$$

where $dp_v^{(j)}(\alpha, \delta)$ is the probability that the jth virtual event originated from (α, δ). The quantity $\overline{Q}$ reaches a maximum if an assumed source position coincides with a real source. It is calculated for each point of the sky, and thus an image of the observed sky region is obtained. This skymap does not use any hypothetical model of the sky. The extent of a source feature on a π-skymap does not reflect the instrument angular resolution; it depends nonlinearly on the number of counts observed from source, background, and other possible sources. The map maximum is interpreted as a strong candidate for a point source, and therefore a source significance analysis; and the determinations of energy spectrum and flux are performed at this position, as described in § IV.

IV. RESULTS

In the upper panel of Figure 4 the π-skymap derived from the first 3.5 hr of the flight is shown. Contour lines are plotted in 10% steps of the maximum value. The likelihood for the existence of a source is maximized at $\alpha = 206°$, $\delta = -43°$, which is close to Cen A.

The asymmetry of the profiles around the source is caused by large off-axis aspect angles of the source and by the special geometrical relation between telescope axis and source during the flight. Under these conditions the image of a source is not expected to be circular. This can be seen in the lower panel of Figure 4, which is the result of a Monte Carlo simulation. In this calculation Cen A ($\alpha = 201°$, $\delta = -43°$) was assumed to be the only γ-ray source in the sky. Gamma-ray emission from this source and its detection in the telescope were simulated under actual balloon flight conditions (atmospheric depth, track and azimuthal orientation of the balloon). The differential photon number spectrum of the source was assumed to be $2 \times 10^{-6}(E/1\ \mathrm{MeV})^{-1.4}\ \mathrm{cm}^{-2}\ \mathrm{s}^{-1}\ \mathrm{keV}^{-1}$ (in agreement with the spectrum derived below). Within statistical uncertainties, the simulated and the measured skymaps are identical; both have the same source signature. This indicates that the measured excess is due to a source at or near the position of Cen A.

The statistical significance of the source detection was determined in the following way: For all events contained in the map, the angular residuals $\rho^{(j)}$ were derived; $\rho^{(j)}$ is defined by $\rho^{(j)} = \bar{\varphi}^{(j)} - \varphi_g^{(j)}$, where $\varphi_g^{(j)}$ is the angle between the source ($\alpha = 201°$, $\delta = -43°$) and the center of the jth event circle $(\alpha_s^{(j)}, \delta_s^{(j)})$ and $\bar{\varphi}^{(j)}$ the derived scatter angle of the jth event.

In the upper panel of Figure 5 the distribution of all angular distances ρ around Cen A is shown for real events (*solid histogram*) and for virtual events (*dashed histogram*). The difference between the two distributions is also indicated. This difference distribution has a maximum at $\rho = 0°$ and a width which corresponds to the angular resolution of the telescope for a point source ($\sim 10°$ FWHM). The excess ($-5° < \rho < +5°$) contains 112 events compared to 329 back-

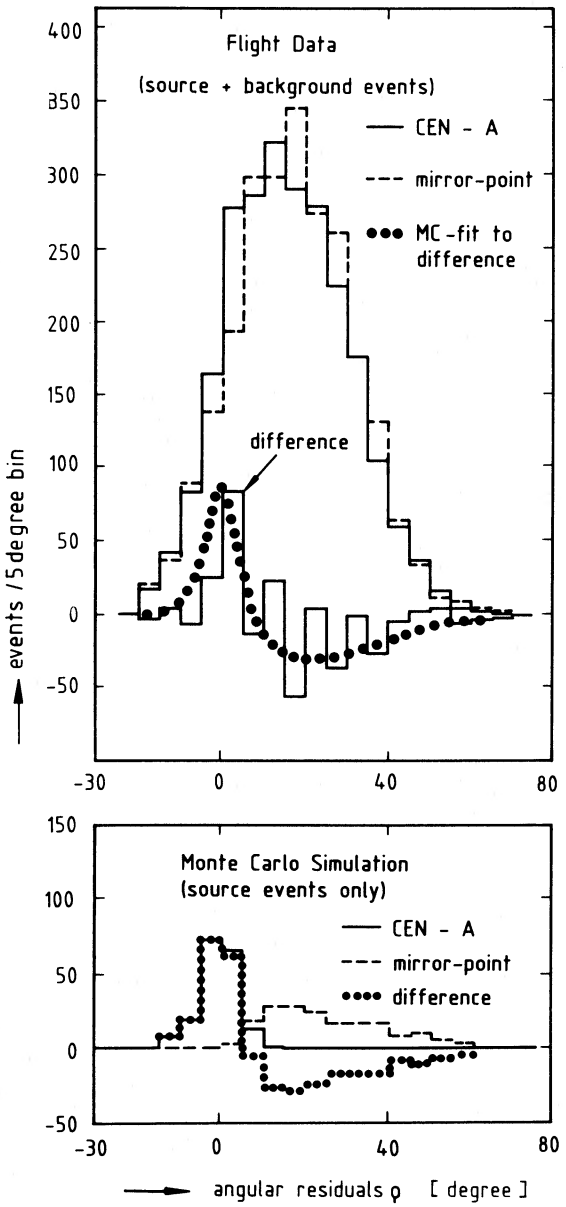

FIG. 5.—Distribution of angular distances around Cen A. (*top*) Flight data (including background); (*bottom*) Monte Carlo simulation (without background).

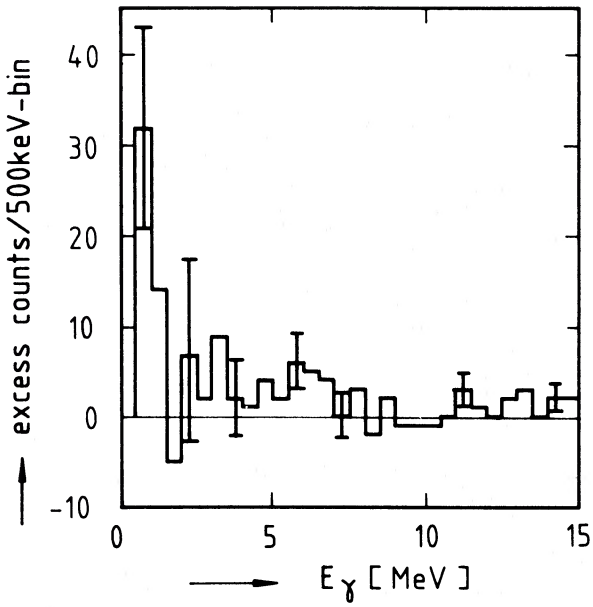

FIG. 6.—Count rate energy spectrum of all source events contained within the excess of Fig. 5 defined by $-4\overset{\circ}{.}5 < \rho < +4\overset{\circ}{.}5$.

ground events and therefore has a statistical significance of 4.0 σ (chance probability: 4×10^{-5}). The signal/background ratio of the source detection is 112/329 = 34%. Azimuthal asymmetries in the 2–10 MeV γ-ray flux at the top of the atmosphere are of the order of only 3%–4% (Ryan *et al.* 1979) and therefore do not affect the source detection.

In the lower panel of Figure 5 the corresponding distributions (around Cen A, around its mirror point, and the difference between the two) are shown for Monte Carlo simulated events originating at Cen A (no background events included). The histogram of the simulation fits the flight data quite well, as is indicated by the dotted curve in the upper panel. The undershoot is caused by the source events, when seen from the mirror point. Its existence is a necessary consequence of the observed excess around $\rho = 0°$. The statistical probability that fluctuations generate a source at the position of Cen A is derived as follows: a bootstrap method analysis (Diaconis and Effron 1983) of the events yields 2.4×10^{-4}. This value is also confirmed by the following argument: the chance probability of the observed excess (4×10^{-5}) is to be multiplied by 6, because $\frac{1}{6}$ of all measured events fall into the internal $-5° < \rho < +5°$.

Figure 6 shows the count rate spectrum of the source events contained in the interval $-4\overset{\circ}{.}5 < \rho < +4\overset{\circ}{.}5$. The distribution of these events over four coarse energy intervals is listed in Table 1. Also listed are the statistical significances for the source detection in each of the four energy intervals. From this table it is clear that the source detection above 3 MeV has the same statistical significances as the detection in the entire 0.7–20 MeV range (4.1 σ).

TABLE 1

COUNT RATE SPECTRUM OF CENTAURUS A

Energy range (MeV)		Significance (σ)	
0.7– 1.5	44 ± 15	2.9	2.5
1.5– 3.0	7 ± 14	0.5	
3.0– 8.0	36 ± 10	3.6	4.1
8.0–20.0	12 ± 6	2.0	
0.7–20.0	99 ± 24	4.1	

The conversion of the count rate spectrum into the differential photon number spectrum is done by means of the Monte Carlo simulation. Trials with different input power-law spectra were made to match the measured count rate spectrum. The resulting γ-ray spectrum is shown in Figure 7. Also shown are

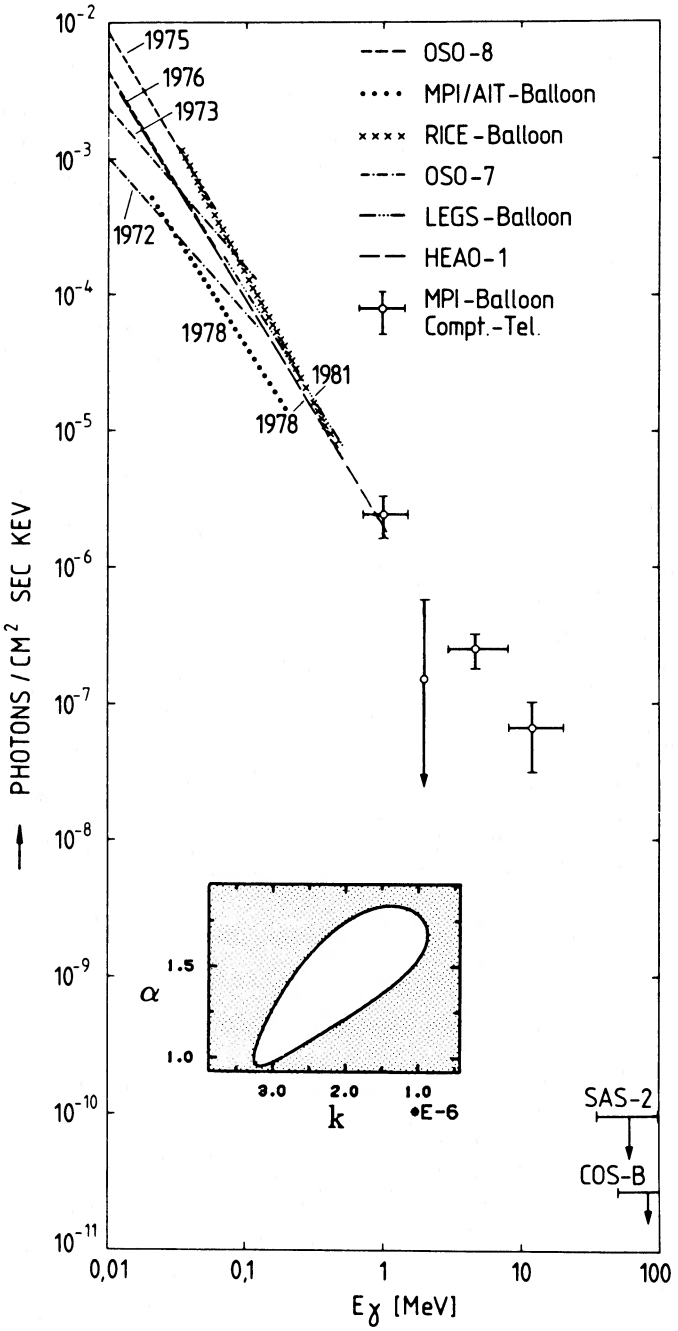

FIG. 7.—Differential photon number spectrum of Cen A at X- and γ-ray energies. The insert shows the 1 σ uncertainties in α and k for a power-law fit to our four data points $k(E/\text{MeV})^{-\alpha}$ cm^{-2} s^{-1} keV^{-1}. The X-ray measurements are from: (*OSO 8*) Mushotzky *et al.* (1978); (MPI/AIT balloon) Pietsch *et al.* (1981); (Rice balloon) Hall *et al.* (1976); (*OSO 7*) Mushotzky *et al.* (1976); (LEGS balloon) Gehrels *et al.* (1984); (*HEAO 1*) Baity *et al.* (1981). The γ-ray limits are from: (*SAS 2*) Bignami *et al.* (1979); (*COS B*) Pollock *et al.* (1981).

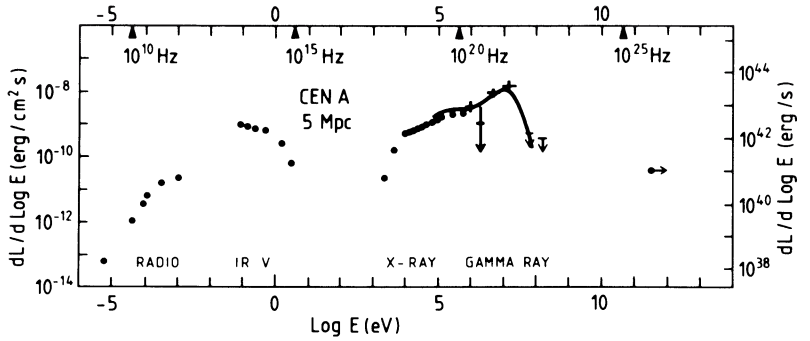

FIG. 8.—Cen A spectrum from radio to γ-ray energies (adopted from Baity *et al.* 1981, with the addition of our results). Also indicated is a fit based on a thermal Comptonization model with $kT_e = 5$ MeV, $\tau_T = 0.15$ (Zdziarski 1985*b*).

the spectra obtained from some hard X-ray measurements and the upper limits derived from *SAS 2* and *COS B* above 35 MeV and 50 MeV. As can be seen our data points lie exactly on the extrapolation of the X-ray spectrum of Cen A. This fact and the position of the observed excess in Figure 4 and the nonexistence of any other known hard X-ray source within 10° of the position of Cen A (see Levine *et al.* 1984) strongly suggests Cen A as the source of the observed γ-ray emission. If our four data points are fitted by a power law of the type $kE_{\mathrm{MeV}}^{-\alpha}$ cm^{-2} s^{-1} keV^{-1}, we obtain $k = (2.2^{+1.1}_{-1.3}) \times 10^{-6}$ and $\alpha = 1.4 \pm 0.4$ (see insert of Fig. 7). Somewhere around 10 MeV, the γ-ray spectrum of Cen A must steepen rapidly in order to meet the limits set by *SAS 2* and *COS B*.

V. DISCUSSION

The main conclusion derived from our measurements is that the energy spectrum of Cen A extends into the MeV region and connects well to the power-law spectrum, which so far has been measured up to several hundred keV. The luminosity of Cen A even peaks at MeV energies, as can be seen from Figure 8, where the luminosity spectrum per decade is plotted over the entire spectral range from radio to γ-ray energies. If the validity of the upper limits derived by *SAS 2* above 35 MeV (Bignami *et al.* 1979) and *COS B* above 50 MeV (Pollock *et al.* 1981) is assumed also for the time of our balloon flight, then the luminosity spectrum must rapidly drop somewhere around 10 MeV.

As the overall source detection is at the 4 σ confidence level only, considerable uncertainties in the single spectral points have to be taken into account when deriving conclusions from the energy spectrum. Three different possible explanations of the spectrum are now discussed: unresolved line emission on top of a continuum spectrum, thermal Comptonization, and synchrotron self-Compton models.

a) Unresolved Line Emission

In principle, the four data points of the derived energy spectrum between 0.7 and 20 MeV are consistent with a spectrum composed of a continuum spectrum, which drops off beyond 1.5 MeV, and of an additional component of unresolved γ-ray lines between 3 and 8 MeV. The detection of two γ-ray lines from Cen A has been reported by Hall *et al.* (1976). The lines are located at 1.6 MeV and 4.5 MeV and have tentatively been identified as excited ^{20}Ne and ^{12}C emission. The existence of these lines is not confirmed by our present data. Our derived 2 σ upper limits are listed in Table 2 together with the line strengths measured by Hall *et al.* (1976) and further upper limits derived by Gehrels *et al.* (1984) and Baity *et al.* (1981).

At present we cannot exclude the possibility that the total observed 3–8 MeV flux is due to a larger number of unresolved lines (of corresponding lower intensity). In this case, however, the luminosity of the lines would be comparable to the total luminosity of the continuum. A much larger continuum luminosity as compared to the line luminosity would be expected, because in the radiating plasma only a small fraction of the total energy loss of the ions is converted into nuclear excitation energy, whereas most of this energy appears as thermal energy of electrons. Though possible ways out of this difficulty have been proposed by Lingenfelter, Higdon, and Ramaty (1978), we prefer the view that the continuum spectrum follows the single power-law shape at least up to ~8 MeV. The next two models are based on this view.

b) Thermal Comptonization Models

One natural explanation for the observed luminosity maximum of Cen A at ~10 MeV and its rapid decrease toward higher photon energies is that the central nucleus of Cen A is powered by infall of matter. As a result of this accretion, the

TABLE 2

γ-RAY LINE EMISSION FROM CENTAURUS A

Reference	Year of Observation	1.6 MeV (cm^{-2} s^{-1})	4.5 MeV (cm^{-2} s^{-1})
Hall *et al.* 1976	1974	$3.4 \pm 1 \times 10^{-3}$	$9.9 \pm 3.0 \times 10^{-4}$
Baity *et al.* 1981[a]	1978	$<4.1 \times 10^{-3}$	...
Gehrels *et al.* 1984[b]	1981	$<6.7 \times 10^{-3}$	4.1×10^{-3}
This experiment	1982	$<3.4 \times 10^{-4}$	8.0×10^{-4}

[a] Corrected in Gehrels *et al.* 1984.
[b] For same line width as measured by Hall *et al.* 1976.

radiating plasma of the nucleus would have to be heated to a temperature corresponding to $kT_e \approx 5$ MeV. It has been shown that power-law X-ray spectra of active galactic nuclei can be produced by Compton collisions of hot plasma electrons with low-energy photons (e.g., infrared photons). The power-law shape is obtained if the number of scattering processes of each photon is sufficiently large. The photon power law drops off at photon energies of a few kT_e, where T_e is the temperature of the electron plasma (for a more recent review of thermal Comptonization models see, e.g., Brinkmann and Trümper 1984).

In the case of Cen A, the thermal electrons ($kT_e \approx 5$ MeV) would have relativistic energies. It has been shown by Pozdnyakov, Sobol', and Sunyaev (1977) and Górecki and Wilozewski (1984) that the Comptonized spectrum in the relativistic case is slightly bumpy because of the superposition of only a few scattering processes, as is schematically illustrated in Figure 9. The photon number spectral index α of a power-law fit to this bumpy spectrum depends on the optical thickness τ_T of the plasma for Thompson scattering. If $\tau_T \ll 1$, then α is approximated by

$$\alpha - 1 = -\frac{\log \tau_T}{\log (16\theta^2)}, \quad (5)$$

where $\theta = kT_e/m_e c^2$.

An acceptable fit to the hard X-ray and low-energy γ-ray spectrum of Cen A, which also meets the upper limits set by *SAS 2* and *COS B* and which is shown in Figure 8, is obtained with $kT_e = 5.1$ MeV and $\tau_T = 0.15$ (Zdziarski 1985*b*). In case of pair equilibrium (pair production = pair annihilation plus pair escape), these two values of T_e and τ_T constrain the dimensionless luminosity l, which is defined by

$$l = \frac{L(>511 \text{ keV})\sigma_T}{Rm_e c^2}, \quad (6)$$

and which corresponds to the compactness parameter L/R. Here L (>511 keV) is the continuum luminosity above 511 keV, σ_T the cross section for Thompson scattering, and R the radius of the radiating plasma sphere. The exact value of l under which pair equilibrium is realized depends on the two model parameters $u = 2n_+/(n_+ + n_-)$ and $\beta = (R/c)/\tau_{esc}$: u is the pair abundance ratio and β is the ratio between light travel time across the source and the pair escape time scale. The maximum value of l is obtained for $u = 1$ and $\beta = 1$ and is of the order of 10 for the parameters of our Cen A spectrum (see Zdziarski 1985*a*, eq. [32]). The value $l = 10$ results in a lower limit to the source radius of 2.5×10^{14} cm.

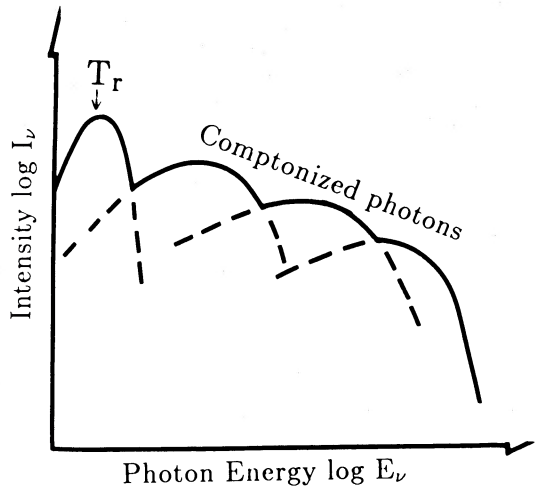

FIG. 9.—Illustration of a typical energy spectrum from multiple Compton scattering of relativistic electrons ($E_e \gg m_e c^2$) with low-energy photons at temperature T_r (according to Pozdnyakov, Sobol', and Sunyaev 1977).

The dip in the measured spectrum between 1.5 and 3 MeV might be explained by a valley between peaks of the thermal Comptonization spectrum. The present measurements are insufficient to derive this conclusion, because of the limited statistical significance of the data points. If, however, the bumpiness of the spectrum is confirmed in an observation with higher sensitivity, the thermal Comptonization model would be proven.

c) *Synchrotron Self-Compton Models*

In these models the existence of nonthermal relativistic electrons in the nuclei of active galaxies is postulated. The electrons produce infrared and radio photons via synchrotron radiation in magnetic fields; the synchrotron photons are then scattered by the same electrons into the X- and γ-ray range. In contrast to the thermal Comptonization models, nonthermal acceleration processes are needed. A possible scenario has been suggested by Protheroe and Kazanas (1983), in which protons undergo first order-Fermi acceleration during infall of matter onto a massive black hole. The required electrons are then produced as secondary particles by nuclear interactions of the protons. A specific synchrotron self-Compton model for Cen A has been suggested by Grindlay (1975). In his two-component model a sharp turnover of the hard X-ray/soft γ-ray spectrum was predicted at ~ 5 MeV in reasonable agreement with the shape derived from our measurements and the *SAS 2* and *COS B* limits. In this model the break at 5 MeV would reflect the observed turnover of the infrared spectrum at frequencies around 10^{14} Hz. The IR turnover would be explained by the high-energy fall-off of the electron spectrum at 1.5 GeV in this specific case.

Another possibility for explaining the break in synchrotron self-Compton models would be photon/photon absorption for sufficiently small sources. Following Herterich (1974), the optical depth $\tau_{\gamma\gamma}(E)$ for photons of energy E is $\tau_{\gamma\gamma}(E) \sim E^{\alpha-1}$, where α again is the photon number spectral index of the production spectrum. If the X- and γ-radiation is uniformly produced within a sphere, then the photon/photon absorption would cause the power-law spectrum to break at some energy E_{br} (defined by $\tau_{\gamma\gamma} = 1$) from proportional to $E^{-\alpha}$ to proportional to $E^{-\alpha}/\tau_{\gamma\gamma}(E) \propto E^{-2\alpha+1}$ (Svensson 1984). For Cen A, $\alpha \approx 1.5$, and hence the γ-ray spectrum at $E > E_{br}$ would steepen by only half a power-law index. This is in contrast to the observations, if the *SAS 2* and *COS B* limits are valid during our balloon flight.

For an inhomogenous source, where the γ-rays are produced in deeper layers than the X-rays, the steepening would be larger, and the spectrum would change from proportional to $E^{-\alpha}$ to proportional to $\exp[-\tau_{\gamma\gamma}(E)]E^{-\alpha}$. This case was discussed in von Ballmoos, Diehl, and Schönfelder (1985). Probably even such a steepening is insufficient to explain the measurements.

The spectral break could also be the consequence of burst-like production of relativistic electrons in the nucleus of Cen A, as was suggested by Pinkau (1980) for the Seyfert galaxy NGC 4151. Because the energy loss time of electrons in Compton

collisions is smaller for high-energy electrons than for low-energy electrons, it produces a time-dependent break in the electron spectrum, resulting in a corresponding break in the γ-ray spectrum. The test of this model requires long-term observations of Cen A, because the break should gradually shift toward lower energies with time.

In general, synchrotron self-Compton models are testable, because they predict correlated intensity changes in the infrared and X-/γ-ray range. Due to the above mentioned energy dependence of the electron lifetime, the delay in the intensity changes should be smaller at γ-ray energies than at X-ray energies.

VI. SUMMARY

γ-ray emission above 700 keV from the direction of Cen A was detected during a balloon flight with the MPI Compton telescope on 1982 October 31. The results were obtained with a new analysis method which provides an efficient means of subtracting instrumental, atmospheric, and cosmic background from the data. The method has similarities with the ON and OFF technique used in X-ray observations, except that our ON and OFF observations are performed simultaneously due to the large field of view of the telescope. The statistical significance of the source detection is 4.1 σ. The location of the source, the profile of the source image in comparison to the one expected from a Monte Carlo simulation of a source at the same position in the sky, and the intensity and shape of the derived energy spectrum strongly indicate that the detected radiation is related to Cen A.

The energy spectrum extends into the MeV range at least up to $\sim$8 MeV and connects well to the power-law spectrum, which so far has been measured up to several hundred keV. Due to statistical limitations, the uncertainties in our single spectral points are quite large. If the upper limits from *SAS 2* and *COS B* above 35 MeV and 50 MeV respectively are assumed to be valid during the time of our observations, then the luminosity maximum of Cen A is at energies around 10 MeV. No γ-ray lines have been found in the spectrum. Our 2 σ upper limits on line emission are below the fluxes reported by Hall *et al.* (1976).

The hard X-ray/soft γ-ray spectrum can be interpreted as a thermal Comptonization spectrum with the parameters $kT_e = 5.1$ MeV and $\tau_T = 0.15$. For the special case of pair equilibrium, a lower limit to the source radius of 2.5×10^{14} cm can be derived from these two values. Our measured spectrum also fits the two-component synchrotron self-Compton model of Grindlay (1975).

The statistical accuracy of the present data is not sufficient to discriminate among the models discussed. Firm conclusions on the radiation mechanism from the energy spectrum require measurements with much better statistics and correlated observation in other spectral ranges. Still, at present it looks very much like the γ-ray photons measured by our telescope were generated by the same process in which they finally ended: Compton collisions. It is certain that Cen A will be one of the very interesting objects to be studied by the Gamma Ray Observatory GRO of NASA, which will allow simultaneous observations of the source over five decades in energy from 100 keV to 10 GeV.

We would like to thank the National Center for Atmospheric Research (NCAR) in the US and the Instituto de Pesquisas Espaciais (INPE) in Brazil for conducting the balloon flight under very difficult conditions. We are grateful to U. Graser, W. Hofmeister, N. Huber, L. Pichl, and F. Schrey from the Max Planck Institute for assistance in our balloon telescope project. We appreciate the support of A. Zdziarski in the discussion of thermal Comptonization models.

REFERENCES

Baity, W. A., *et al.* 1981, *Ap. J.*, **244**, 429.
Bignami, G. F., Fichtel, C. E., Hartman, R. C., and Thompson, D. J. 1979, *Ap. J.*, **232**, 649.
Bowyer, D. S., Lampton, M., Mack, J., and de Mendonca, F. 1970, *Ap. J. (Letters)*, **161**, L1.
Brinkmann, W., and Trümper, J., ed. 1984, *X-Ray and UV-Emission from Active Galactic Nuclei* (MPE Rept., No. 184).
Diaconis, P., and Effron, B. 1983, *Sci. Am.*, Vol. **248**, No. 5 (May), 96.
Gehrels, N., Cline, T. L., Teegarden, B. J., Paciesas, W. S., Tueller, J., Durouchoux, Ph., and Hameury, J. M. 1984, *Ap. J.*, **278**, 112.
Górecki, A., and Wilozewski, W. 1984, *Acta Astr.*, **34**, 141.
Graser, U., and Schönfelder, V. 1982, *Ap. J.*, **263**, 677.
Grindlay, J. 1975, *Ap. J.*, **199**, 49.
Grindlay, J., Helmken, H. F., Hanbury Brown, R., Davis, J., and Allen, L. R. 1975, *Ap. J. (Letters)*, **197**, L9.
Hall, k. D., Meegan, C. A., Walraven, G. D., Djuth, F. T., and Haymes, R. C. 1976, *Ap. J.*, **210**, 631.
Herterich, K. 1974, *Nature*, **250**, 311.
Levine, A. M., *et al.* 1984, *Ap. J. Suppl.*, **54**, 581.
Lingenfelter, R. E., Higdon, J. C., and Ramaty, R. 1978, in *Gamma Ray Spectroscopy in Astrophysics*, ed. T. L. Cline and R. Ramaty (NASA TM 79619), p. 252.
Mushotzky, R. F., Baity, W. A., Wheaton, W. A., and Peterson, L. E. 1976, *Ap. J. (Letters)*, **206**, L45.
Mushotzky, R. F., Serlemitsos, R. H., Becker, H., Boldt, A., and Holt, S. S. 1978, *Ap. J.*, **220**, 790.
Pietsch, W., Reppin, C., Trümper, J., Voges, W., Lewin, W., Kendziorra, E., and Staubert, R. 1981, *Astr. Ap.*, **94**, 234.
Pinkau, K., 1980, *Astr. Ap.*, **87**, 192
Pollock, A. M. T., *et al.* 1981, *Astr. Ap.*, **94**, 116.
Pozdnyakov, L. A., Sobol', I. M., and Sunyaev, R. A. 1977, *Soviet Astr.*, **21**, 708.
Protheroe, R. J., and Kazanas, D. 1983, *Ap. J.*, **265**, 620.
Ryan, J. M., Jennings, M. C., Badwin, M. D., Zych, A. D., and White, R. S. 1979, *J. Geophys. Res.*, **84**, 5279.
Schönfelder, V., Graser, U., and Diehl, R. 1982, *Astr. Ap.*, **110**, 138.
Svensson, R. 1984, in *X-Ray and UV-Emission from Active Galactic Nuclei*, ed. W. Brinkmann and J. Trümper (MPE Rept., No. 184), p. 152.
von Ballmoos, P., Diehl, R., and Schönfelder, V. 1985, in *Proc. 19th Internat. Cosmic Ray Conf.* (La Jolla), (NASA CP 2376) **1**, 273.
———. 1986, *Adv. Space Res.*, in press.
Zdziarski, A. A. 1985*a*, *Ap. J.*, **289**, 514.
———. 1985*b*, private communication.

PETER VON BALLMOOS, ROLAND DIEHL, and VOLKER SCHÖNFELDER: Max-Planck-Institut für extraterrestrische Physik, 8046 Garching, Federal Republic of Germany